Buckling analysis of a microbeam embedded in an elastic medium with deformable boundary conditions

Mustafa Özgür Yayli ✉

Faculty of Engineering, Department of Civil Engineering, Uludag University, 16059 Görükle Kampüsü, BURSA, Turkey
✉ *E-mail: ozguryayli@uludag.edu.tr*

Published in Micro & Nano Letters; Received on 6th May 2016; Revised on 21st July 2016; Accepted on 25th July 2016

The buckling of elastically restrained embedded microbeam under axial compression load is researched. The effects of small size, axial compression load and surrounding elastic medium are taken into account at the same time. Winkler elastic foundation approach is used to simulate the interaction between microbeam and elastic medium. Fourier sine series is employed for the simulation of microbeam deflections. A coefficient matrix is obtained with the aid of applying Stokes' transformation to corresponding boundary conditions. The buckling characteristics of elastically restrained embedded microbeams are investigated in some numerical examples. There are very good agreements between this study and the previous results indicating the validity of the presented method.

1. Introduction: Microbeams have been widely used in nano and micro-electro-mechanical systems. The characteristic dimensions of microbeams are typically on the order of microns and sub-microns. It has been shown in some experimental studies that the structures become stiffer in smaller sizes [1–3]. The experimental results reveal that classical elasticity theories do not have the ability to predict the size-dependent deformation behaviour of nano- and micro-sized structures. In order to be able to understand the mechanical behaviours of these structures, several non-classical continuum theories have been developed such as micropolar theory [4], couple stress theory [5–7], strain gradient theories [8, 9] and non-local elasticity theory [10, 11].

Non-local elasticity theory states that stresses at a reference point are a function not only of the strains at that point but also a function of the strains at every points in the domain [11]. This theory is a popular technique for modelling mechanical behaviour of carbon nanotubes (CNT) [12, 13]. Reddy and Pang [14] have presented Timoshenko beam and the Euler-Bernoulli theories using the non-classical constitutive relations of Eringen [11]. Some of researchers have investigated the static behaviours of single walled, double and multi-walled CNT such as [15, 16]. Pradhan and Murmu [17] have presented a single non-local beam model to investigate the static and dynamic characteristics of a nanocantilever beam. Dynamical behaviour of CNT embedded in an elastic medium has been examined by some researchers such as [18, 19]. Free vibration behaviour of CNTs have been considered by some researchers [20, 21]. Free axial vibration of the nanorods has been considered by Aydogdu [22]. The small size effects on free axial vibrations of heterojunction CNTs based on the classical and non-classical rod theories have been investigated by Filiz and Aydogdu [23].

Yang *et al.* [24] have proposed the modified couple stress theory in which only one material length scale parameter is introduced. Thereafter, the modified couple stress and strain gradient elasticity theories have been widely applied to the static, stability, and dynamic analysis of microbeams [25–27].

A short review of literature reveals that most of the theoretical works devoted to the buckling problem are based on the assumptions that the boundary conditions are non-deformable. In this work, stability analysis of embedded microbeam with deformable boundary conditions is performed. Fourier sine series is employed for the simulation of microbeam deflections. A coefficient matrix is obtained with the aid of applying Stokes' transformation to corresponding boundary conditions. A detailed parametric study is performed to indicate influences of material length scale parameter, spring and Winkler parameter on critical buckling loads of embedded microbeams. There are very good agreements between this study and the previous results indicating the validity of the presented method.

2. Problem definition and modelling: It can be noted that the microbeams could be used as atomic force microscope (see Fig. 1). During an experiment, micro-sized samples may behave as attached linear spring to the testing device and this may affect the buckling (stability) behaviour of the atomic force microscope.

Unfortunately, the previous gradient elasticity beam models based on Euler Bernoulli beam theory mostly faces the following problem: The well-known gradient elasticity models are mostly based on microbeams with rigid boundary conditions (simply supported, clamped-clamped, clamped-pinned). There are only a few reports on the microbeams with restrained boundary conditions. However, in practical engineering, the end supports of microbeam is not limited to rigid boundary conditions. In this work, elastic buckling behaviour of size dependent microbeams resting on elastic foundation under deformable boundary conditions is studied based on a gradient elasticity theory. Consider a microbeam which is subjected to an in-plane axial load P, and the both side of the microbeam is movable in a vertical direction.

Strain gradient elasticity theory proposed by Papargyri-Beskou *et al.* [28] is used in this Letter. According to this theory, the governing differential equation of a microbeam embedded in elastic medium is given by

$$EI\frac{d^4w}{\partial x^4} - EI\gamma^2\frac{d^6w}{\partial x^6} + P\frac{d^2w}{\partial x^2} + kw = 0 \tag{1}$$

where x is an independent variable, w denotes the vertical displacement of the microbeam. EI is the flexural stiffness of the microbeam and γ is the material scale parameter. I represents the moment of inertia, k represent the constant of the foundation, known as Winkler's constant. The microbeam is made of homogeneous isotropic linearly elastic material with Youngs' modulus E (Fig. 2).

3. Modal displacement function: In the strain gradient elasticity, Fourier sine series expansion together with Stokes' transformation will be used to represent the lateral deflection of microbeam. This method gives more flexibility to treat deformable boundary conditions. The modal displacement function $W(x)$ which is

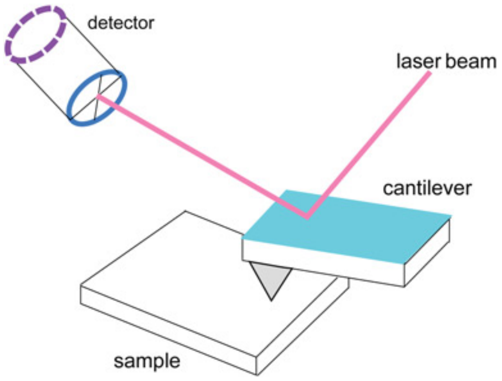

Fig. 1 *Schematic drawing of atomic force microscope*

analytically equal to vertical displacement $w(x)$ of the microbeam is described in three separate regions, two for supporting points and the other for the intermediate places between the supporting points

$$w(x) = W_0 \quad x = 0, \tag{2}$$

$$w(x) = W_L \quad x = L, \tag{3}$$

$$w(x) = W(x) = \sum_{n=1}^{\infty} A_n \sin\left(\frac{n\pi x}{L}\right) \quad 0 < x < L, \tag{4}$$

with

$$A_n = \frac{2}{L}\int_0^L W(x)\sin\left(\frac{n\pi x}{L}\right)\mathrm{d}x. \tag{5}$$

It should be noted that the two boundary points, $x = 0$ and $x = L$, have been excluded in (4) since the Fourier sine series may not converge to the true displacement values in the boundary points. Equations (2) and (3) allow freedom in choosing the lateral displacement function. Term wise differentiation of (4) yields

$$W'(x) = \sum_{n=1}^{\infty}\frac{n\pi}{L}A_n\cos\left(\frac{n\pi x}{L}\right), \tag{6}$$

$W'(x)$ can be represented by a Fourier cosine series

$$W'(x) = \frac{b_0}{L} + \sum_{n=1}^{\infty} b_n\cos\left(\frac{n\pi x}{L}\right). \tag{7}$$

The coefficients (b_0, b_n) in (7) are given by

$$b_0 = \frac{2}{L}\int_0^L W'(x)\,\mathrm{d}x = \frac{2}{L}\left[W(L) - W(0)\right], \tag{8}$$

$$b_n = \frac{2}{L}\int_0^L W'(x)\cos\left(\frac{n\pi x}{L}\right)\mathrm{d}x \quad n = 1, 2\ldots, \tag{9}$$

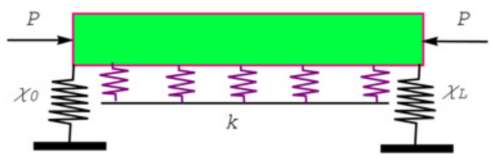

Fig. 2 *Microbeam embedded in an elastic medium with deformable boundary conditions*

by applying integration by parts

$$b_n = \frac{2}{L}\left[W(x)\cos\left(\frac{n\pi x}{L}\right)\right]_0^L + \frac{2}{L}\left[\frac{n\pi}{L}\int_0^L W(x)\sin\left(\frac{n\pi x}{L}\right)\mathrm{d}x\right], \tag{10}$$

$$b_n = \frac{2}{L}\left[(-1)^n W(L) - W(0)\right] + \frac{n\pi}{L}A_n. \tag{11}$$

The above procedure is known as Stokes' transformation. To compute the series expressions for the higher order derivatives of a Fourier sine series, Stokes' transformation should be utilised. The present solution method (Fourier series and Stokes' transformation) will be helpful when dealing with microbeams with deformable conditions. The first-sixth derivatives of $W(x)$ can be determined by applying Stokes' transformation as follows

$$\frac{\mathrm{d}W(x)}{\mathrm{d}x} = \frac{W_L - W_0}{L} + \sum_{n=1}^{\infty}\cos(\alpha_n x)\left(\frac{2((-1)^n W_L - W_0)}{L} + \alpha_n A_n\right), \tag{12}$$

$$\frac{\mathrm{d}^2 W(x)}{\mathrm{d}x^2} = -\sum_{n=1}^{\infty}\alpha_n\sin(\alpha_n x) \times \left(\frac{2((-1)^n W_L - W_0)}{L} + \alpha_n A_n\right), \tag{13}$$

$$\frac{\mathrm{d}^3 W(x)}{\mathrm{d}x^3} = \frac{W_L'' - W_0''}{L} + \sum_{n=1}^{\infty}\cos(\alpha_n x)\left(\frac{2((-1)^n W_L'' - W_0'')}{L} - \alpha_n^2\left(\frac{2((-1)^n\psi_L - \psi_0)}{L} + \alpha_n A_n\right)\right), \tag{14}$$

$$\frac{\mathrm{d}^4 W(x)}{\mathrm{d}x^4} = -\sum_{n=1}^{\infty}\alpha_n\sin(\alpha_n x)\left(\frac{2((-1)^n W_L'' - W_0'')}{L} - \alpha_n^2\left(\frac{2((-1)^n W_L - W_0)}{L} + \alpha_n A_n\right)\right), \tag{15}$$

$$\frac{\mathrm{d}^5 W(x)}{\mathrm{d}x^5} = \frac{W_L'''' - W_0''''}{L} + \sum_{n=1}^{\infty}\cos(x\alpha_n)\left(\alpha_n^4\left(\frac{2((-1)^n W_L - W_0)}{L} + \alpha_n A_n\right) - \frac{2\alpha_n^2((-1)^n W_L'' - W_0'')}{L} + \frac{2((-1)^n W_L'''' - W_0'''')}{L}\right), \tag{16}$$

$$\frac{\mathrm{d}^6 W(x)}{\mathrm{d}x^6} = -\sum_{n=1}^{\infty}\alpha_n\sin(x\alpha_n) \times \left(\alpha_n^4\left(\frac{2((-1)^n W_L - W_0)}{L} + \alpha_n A_n\right) - \frac{2\alpha_n^2((-1)^n W_L'' - W''{}_0)}{L} + \frac{2((-1)^n W_L'''' - W_0'''')}{L}\right), \tag{17}$$

where

$$\alpha_n = \frac{n\pi}{L}. \tag{18}$$

The main objective is to seek series solutions for the displacements. To do this, the Fourier coefficients which simultaneously satisfy the governing equation need to be determined. Therefore, substituting

doi: 10.1049/mnl.2016.0257

(4), (13), (15) and (17) into (1), the Fourier coefficients A_n can be written in terms of different parameters as follows

$$A_n = \frac{2\alpha_n\left(-\tilde{B}_n + (-1)^n\left(EI\tilde{\varphi}_n + W_L\tilde{P}_\eta\right) + W_0\tilde{P}_\psi\right)}{L\tilde{P}_\xi}, \tag{19}$$

where

$$\tilde{B}_n = \gamma^2 EIW_0'''' + W_0''\left(\gamma^2 EI\alpha_n^2 + EI\right), \tag{20}$$

$$\tilde{\varphi}_n = -\gamma^2 W_L'''' + \gamma^2 W_L''\alpha_n^2 + W_L'', \tag{21}$$

$$\tilde{P}_\eta = P - EI\alpha_n^2\left(\gamma^2\alpha_n^2 + 1\right), \tag{22}$$

$$\tilde{P}_\psi = \gamma^2 EI\alpha_n^4 + EI\alpha_n^2 - P, \tag{23}$$

$$\tilde{P}_\xi = \gamma^2 EI\alpha_n^6 + EI\alpha_n^4 + k - P\alpha_n^2. \tag{24}$$

The lateral displacement function of a microbeam having no axial restraints at both ends becomes

$$W = \sum_{n=1}^{\infty} \frac{2\alpha_n(-\tilde{B}_n + (-1)^n(EI\tilde{\varphi}_n + W_L\tilde{P}_\eta) + W_0\tilde{P}_\psi)}{L\tilde{P}_\xi} \times \sin(\alpha_n x). \tag{25}$$

It should be note that the above equation is reduced to that of the classical relation wherein the small scale parameter is set to zero.

4. Boundary conditions: A microbeam of length L and with deformable boundary conditions is considered as in Fig. 1. Based on the strain gradient elasticity it is then seen that the following force boundary conditions at the spring locations can be written as

$$\chi_0 W_0 = P\frac{\mathrm{d}W}{\mathrm{d}x} - EI\left(\frac{\mathrm{d}^3W}{\mathrm{d}x^3} - \gamma^2\frac{\mathrm{d}^5W}{\mathrm{d}x^5}\right), \quad x = 0, \tag{26}$$

$$\chi_L W_L = P\frac{\mathrm{d}W}{\mathrm{d}x} - EI\left(\frac{\mathrm{d}^3W}{\mathrm{d}x^3} - \gamma^2\frac{\mathrm{d}^5W}{\mathrm{d}x^5}\right), \quad x = L, \tag{27}$$

where χ_0 and χ_L denote the stiffnesses of the springs at the ends of the microbeam. Moreover, the other boundary conditions are also presented as [28, 29]

$$W_0'' = W_0'''' = 0, \quad x = 0, \tag{28}$$

$$W_L'' = W_L'''' = 0, \quad x = L. \tag{29}$$

After some mathematical manipulations, the substitution of (12), (14), (16) and (19) into (26)–(29) leads to the two homogeneous simultaneous equations

$$\left(\tilde{P}_b + \tilde{\chi}_0 + \sum_{n=1}^{\infty}\frac{2K\left(\tilde{P}_b + \pi^4\delta^2n^4 + \pi^2n^2\right)}{-\pi^2n^2\tilde{P}_b + K + \pi^6\delta^2n^6 + \pi^4n^4}\right)W_0 + \left(-\tilde{P}_b - \sum_{n=1}^{\infty}\frac{2K(-1)^n\left(\tilde{P}_b + \pi^4\delta^2n^4 + \pi^2n^2\right)}{-\pi^2n^2\tilde{P}_b + K + \pi^6\delta^2n^6 + \pi^4n^4}\right)W_L = 0, \tag{30}$$

$$\left(-\tilde{P}_b - \sum_{n=1}^{\infty}\frac{2K(-1)^n\left(\tilde{P}_b + \pi^4\delta^2n^4 + \pi^2n^2\right)}{-\pi^2n^2\tilde{P}_b + K + \pi^6\delta^2n^6 + \pi^4n^4}\right)W_0 + \left(\tilde{P}_b + \tilde{\chi}_L + \sum_{n=1}^{\infty}\frac{2K\left(\tilde{P}_b + \pi^4\delta^2n^4 + \pi^2n^2\right)}{-\pi^2n^2\tilde{P}_b + K + \pi^6\delta^2n^6 + \pi^4n^4}\right)W_L = 0, \tag{31}$$

where

$$\delta = \frac{\gamma}{L}, \tag{32}$$

$$\tilde{P}_b = \frac{PL^2}{EI}, \tag{33}$$

$$K = \frac{kL^3}{EI}, \tag{34}$$

$$\tilde{\chi}_0 = \frac{\chi_0 L^3}{EI}, \tag{35}$$

$$\tilde{\chi}_L = \frac{\chi_L L^3}{EI}, \tag{36}$$

where $\tilde{\chi}_0$ and $\tilde{\chi}_L$ are the dimensionless stiffnesses of springs. If $\tilde{\chi}_0$ and $\tilde{\chi}_L$ approache 0, these boundaries degenerate to free ends, while if $\tilde{\chi}_0$ and $\tilde{\chi}_L$ approache infinity, they degenerate to simply supported ends. One can obtain the following system of linear equations in matrix form to be solved for the constants (W_0, W_L)

$$\begin{bmatrix} \phi_{11} & \phi_{12} \\ \phi_{21} & \phi_{22} \end{bmatrix}\begin{bmatrix} W_0 \\ W_L \end{bmatrix} = 0, \tag{37}$$

where

$$\phi_{11} = \tilde{P}_b + \tilde{\chi}_0 + \sum_{n=1}^{\infty}\frac{2K\left(\tilde{P}_b + \pi^4\delta^2n^4 + \pi^2n^2\right)}{-\pi^2n^2\tilde{P}_b + K + \pi^6\delta^2n^6 + \pi^4n^4}, \tag{38}$$

$$\phi_{12} = -\tilde{P}_b - \sum_{n=1}^{\infty}\frac{2K(-1)^n\left(\tilde{P}_b + \pi^4\delta^2n^4 + \pi^2n^2\right)}{-\pi^2n^2\tilde{P}_b + K + \pi^6\delta^2n^6 + \pi^4n^4}, \tag{39}$$

$$\phi_{21} = -\tilde{P}_b - \sum_{n=1}^{\infty}\frac{2K(-1)^n\left(\tilde{P}_b + \pi^4\delta^2n^4 + \pi^2n^2\right)}{-\pi^2n^2\tilde{P}_b + K + \pi^6\delta^2n^6 + \pi^4n^4}, \tag{40}$$

$$\phi_{22} = \tilde{P}_b + \tilde{\chi}_L + \sum_{n=1}^{\infty}\frac{2K\left(\tilde{P}_b + \pi^4\delta^2n^4 + \pi^2n^2\right)}{-\pi^2n^2\tilde{P}_b + K + \pi^6\delta^2n^6 + \pi^4n^4}. \tag{41}$$

Equation (37) defines an eigenvalue problem. The critical buckling loads can be computed by setting the following determinant to zero.

$$\left|\phi_{ij}\right| = 0 \quad (i, j = 1, 2). \tag{42}$$

The characteristic equation of above determinant can be solved by assigning the different values of $\tilde{\chi}_0$ and $\tilde{\chi}_L$ corresponding to the end springs.

5. Results and discussions: In this section, some numerical examples will be presented. The accuracy and validity of the suggested method is checked by comparing the calculated results with those given in the literature. Moreover, the effects of the main parameters including Winkler modulus, the small scale parameter and the boundary conditions on the critical buckling loads of the microbeam are also studied. A computer code is developed in MATLAB based on (42). As eigenvalues of coefficient matrix are sensitive to truncated terms, a convergence test is performed to determine the minimum number of terms required to obtain accurate results for (42). In this numerical validation, the critical buckling loads are obtained by present approach using the first 150 terms of the infinite series. The small scale parameter of the microbeam is $\delta = 0$, 1/20, 1/10 and the spring parameters at the ends are taken as ($\tilde{\chi}_0 = \tilde{\chi}_L = 10^5$) for simple supported case. It is observed from Table 1 that when the stiffnesses of springs are infinitely large ($\tilde{\chi}_0 = \tilde{\chi}_L = 10^5$), the results are exactly match with those reported by Artan and

Table 1 Comparison of the critical buckling loads of simple supported microbeam obtained using gradient elasticity theory

δ	Simple supported microbeam		$\tilde{\chi}_0 = \tilde{\chi}_L = 10^5$
	Ref. [29]	Ref. [30]	Present
		$\sqrt{\bar{P}}$	$\sqrt{\tilde{P}_b}$
0	3,1416	3,1416	3,1416
$\frac{1}{20}$	3.1801	3.1801	3,1801
$\frac{1}{10}$	3.2930	3.2930	3.2930

Table 2 Effect of elastic medium and small scale parameters on the critical buckling parameter of microbeam

	δ					
K	0	$\frac{1}{20}$	$\frac{1}{15}$	$\frac{1}{10}$	$\frac{1}{7}$	$\frac{1}{5}$
1	9971	10,215	10,404	10,945	11,959	13,867
3	10,174	10,417	10,610	11,148	12,162	14,070
5	10,377	10,620	10,811	11,351	12,365	14,273
7	10,579	10,823	11,012	11,554	12,567	14,476
10	10,884	11,127	11,317	3,110	12,872	14,780
13	11,188	11,431	11,621	11,858	13,176	15,084

Toksoz [29]. According to Table 1, present analytical solution is convergent. From this table it is clearly seen that 150 terms of infinite series are sufficient to obtain the accurate results for the present analysis.

To more clarify the convergence of the critical buckling load parameter $\tilde{P}_b$, the analytical results for different elastic medium parameter and small scale parameter are listed in Table 2. The spring parameters $\tilde{\chi}_0 = \tilde{\chi}_L = 10^5$ are considered in the computation. Table 2 obviously indicates that the elastic medium parameter K has an important influence on the critical buckling loads. The increasing rates of the critical buckling loads become faster by increasing in the small scale parameter.

To investigate the effects of the small scale parameter on the critical buckling loads, variation of normalised critical buckling loads with K values are schematically plotted in Fig. 3 for various values of elastic medium parameters. Based on the results in Fig. 3, the increasing value of the elastic medium parameter leads to an increase in the magnitude of critical buckling load. As expected, the stiffening effect of elastic medium parameter is to increase the critical buckling load. The increasing value of small scale parameter (δ) leads to an increase the buckling load.

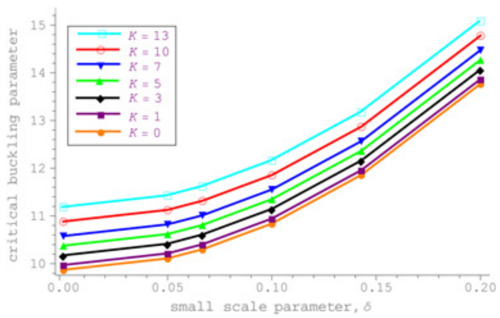

Fig. 3 *Effects of small scale parameter for different elastic medium parameter*

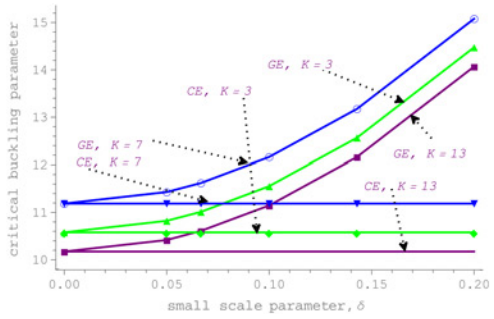

Fig. 4 *Comparisons between classical and gradient elasticity results*

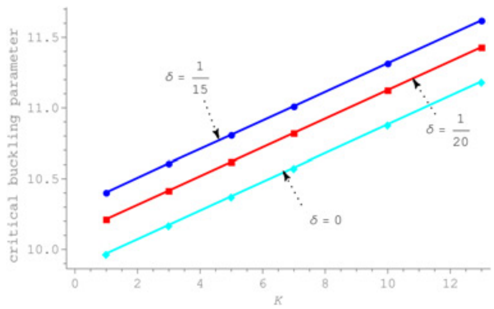

Fig. 5 *Effects of elastic medium for different small scale parameter (δ = 0, 1/20, 1/15)*

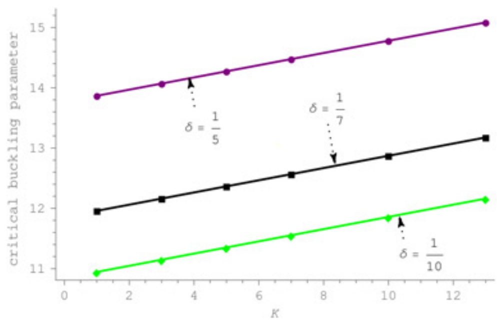

Fig. 6 *Effects of elastic medium for different small scale parameter (δ = 1/10, 1/7, 1/5)*

Comparisons between classical and gradient elasticity results are presented in Fig. 4. The index *CE* denotes classical elasticity and the index *GE* denotes gradient elasticity. The increasing value of length scale parameter leads to an increase in the magnitude of critical buckling load. It is noted from Fig. 4 that if a microbeam is

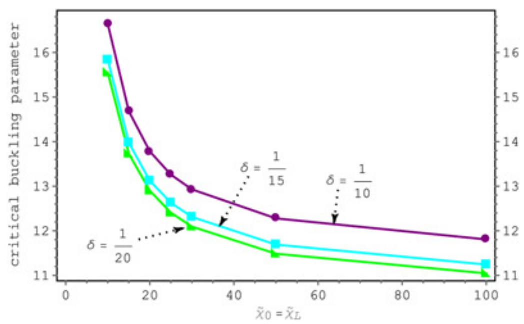

Fig. 7 *Effects of dimensionless spring parameters at the ends for different small scale parameter (δ = 0, 1/20, 1/15)*

doi: 10.1049/mnl.2016.0257

rested on Winkler's elastic medium with length scale parameter $\delta = \gamma/L = 0$, the critical buckling load is constant with respect to the variation of length scale parameter-to-length ratio.

The effects of Winkler's elastic medium on the critical buckling load parameter is presented in Figs. 5 and 6 for a microbeam with $\delta = 0$, 1/20, 1/15, 1/10, 1/7, 1/5 and $\tilde{\chi}_0 = \tilde{\chi}_L = 10^5$. The increasing value of the elastic medium parameter increases the stiffness of the microbeam. It can be seen that increasing value of the small scale parameter leads to an increase in the magnitude of dimensionless critical buckling load.

To illustrate the effect of spring parameters at the ends on buckling responses of microbeam, Fig. 7 plots the critical buckling loads with respect to dimensionless material length scale parameter for a elastically restrained microbeam with $K = 5$. The increasing value of the spring parameters leads to a decrease in the magnitude of critical buckling load. It is also seen that the small scale effects are more significant for large $\delta = \gamma/L$ values when compared with small ones.

6. Conclusion: On the basis of the gradient elasticity theory, an analytical approach is presented for the stability analysis of embedded microbeams with deformable boundary conditions. The lateral displacement function is sought as the superposition of a Fourier sine series and Stokes' transformation that is used to take care of the deformable boundary conditions. The validity of this method is established for simple supported boundary conditions. Various boundary conditions are considered and solved in several parametric examples. The influence of the small scale parameter and end springs on the critical buckling loads is examined in some numerical examples. It can be concluded that the small scale effects are significant when the microbeam length to the length scale parameter ratio is a small quantity.

7 References

[1] Poole W.J., Ashby M.F., Fleck N.A.: 'Micro-hardness of annealed and work-hardened copper polycrystals', *Scr. Mater.*, 1996, **34**, pp. 559–564

[2] Lam D.C.C., Yang F., Chong A.C.M., *et al.*: 'Experiments and theory in strain gradient elasticity', *J. Mech. Phys. Solids*, 2003, **51**, pp. 1477–1508

[3] McFarland A.W., Colton J.S.: 'Role of material microstructure in plate stiffness with relevance to microcantilever sensors.', *J. Micromech. Microeng.*, 2005, **15**, pp. 1060–1067

[4] Eringen A.C.: 'Theory of micropolar plates', *Z. Angew. Math. Phys.*, 1967, **18**, pp. 12–30

[5] Mindlin R.D., Tiersten H.F.: 'Effects of couple-stresses in linear elasticity', *Arch. Ration. Mech. Anal.*, 1962, **11**, pp. 415–448

[6] Koiter W.T.: 'Couple stresses in the theory of elasticity I and II', *Proc. K. Ned. Akad. Wet. B*, 1964, **67**, pp. 17–44

[7] Toupin R.A.: 'Theory of elasticity with couple stresses', *Arch. Ration. Mech. Anal.*, 1964, **17**, pp. 85–112

[8] Fleck N.A., Hutchinson J.W.: 'A phenomenological theory for strain gradient effects in plasticity', *J. Mech. Phys. Solids*, 1993, **41**, pp. 1825–1857

[9] Fleck N.A., Hutchinson J.W.: 'A reformulation of strain gradient plasticity', *J. Mech. Phys. Solids*, 2001, **49**, pp. 2245–2271

[10] Eringen A.C.: 'On differential equations of nonlocal elasticity and solutions of screw dislocation and surface-waves', *J. Appl. Phys.*, 1983, **54**, pp. 4703–4710

[11] Eringen A.C., Edelen D.G.B.: ' On nonlocal elasticity', *Int. J. Eng. Sci.*, 1972, **10**, pp. 233–248

[12] Sudak L.J.: 'Column buckling of multiwalled carbon nanotubes using nonlocal continuum mechanics', *J. Appl. Phys.*, 2003, **94**, pp. 7281–7287

[13] Peddieson J., Buchanan G.R., McNitt R.P.: 'Application of nonlocal continuum models to nanotechnology', *Int. J. Eng. Sci.*, 2003, **41**, pp. 305–312

[14] Reddy J.N., Pang S.D.: 'Nonlocal continuum theories of beam for the analysis of carbon nanotubes', *J. Appl. Phys.*, 2008, **103**, pp. 1–16

[15] Wong E.W., Sheehan P.E., Lieber C.M.: 'Nanobeam mechanics: elasticity, strength and toughness of nanorods and nanotubes', *Science*, 1997, **277**, pp. 1971–1975

[16] Arash B., Wang Q.: 'A review on the application of nonlocal elastic models in modeling of carbon nanotubes and graphenes', *Comput. Mater. Sci.*, 2012, **51**, pp. 303–313

[17] Pradhan S.C., Murmu T.: 'Buckling of single layer graphene sheet based on nonlocal elasticity and higher order shear deformation theory', *Phys. Lett. A*, 2010, **373**, pp. 4182–4188

[18] Bachtold A., Hadley P., Nakanihi T., *et al.*: 'Logic circuits with carbon nanotube transistors', *Science*, 2001, **294**, pp. 1317–1320

[19] Kiani K.: 'A meshless approach for free transverse vibration of embedded single-walled nanotubes with arbitrary boundary conditions accounting for nonlocal effect', *Int. J. Mech. Sci.*, 2010, **52**, pp. 1343–1356

[20] Ece M.C., Aydogdu M.: 'Nonlocal elasticity effect on vibration of in-plane loaded double-walled carbon nano-tubes', *Acta Mech.*, 2007, **190**, pp. 185–195

[21] Simsek M.: 'Vibration analysis of a single-walled carbon nanotube under action of a moving harmonic load based on nonlocal elasticity theory', *Phys.-E Low-dimens. Syst. Nanostructures*, 2010, **43**, pp. 182–191

[22] Aydogdu M.: 'Axial vibration of the nanorods with the nonlocal continuum rod model', *Phys.-E Low-dimens. Syst. Nanostructures*, 2009, **41**, pp. 861–864

[23] Filiz S., Aydogdu M.: 'Axial vibration of carbon nanotube heterojunctions using nonlocal elasticity', *Comput. Mater. Sci.*, 2010, **49**, pp. 619–627

[24] Yang F., Chong A.C.M., Lam D.C., *et al.*: 'Couple stress based strain gradient theory for elasticity', *Int. J. Solids Struct.*, 2002, **39**, pp. 2731–2743

[25] Park S.K., Gao X.L.: 'Bernoulli-Euler beam model based on a modified couple stress theory', *J. Micromech. Microeng.*, 2006, **16**, pp. 2355–2359

[26] Ma H.M., Gao X.L., Reddy J.N.: 'A microstructure dependent Timoshenko beam model based on a modified couple stress theory', *J. Mechan. Phys. Solids*, 2008, **56**, pp. 3379–3391

[27] Simsek M.: 'Dynamic analysis of an embedded microbeam carrying a moving microparticle based on the modified couple stress theory', *Int. J. Eng. Sci.*, 2010, **48**, pp. 1721–1732

[28] Papargyri-Beskou S., Tsepoura K.G., Polyzos D., *et al.*: 'Bending and stability analysis of gradient elastic beams', *Int. J. Solids Struct.*, 2003, **40**, pp. 385–400

[29] Artan R., Toksoz A.: 'Stability analysis of gradient elastic beams by the method of initial value', *Arch. Appl. Mech*, 2011, **18**, pp. 347–351

[30] Yayli M.O.: 'Stability analysis of gradient elastic microbeams with arbitrary boundary conditions', *J. Mechan. Sci. Technol.*, 2015, **29**, pp. 3373–3380

doi: 10.1049/mnl.2016.0257